



HAL
open science

Dynamic invariance in near field acoustic levitation

Nicolas Elie, Antoinette Blouin, Noël Brunetière

► **To cite this version:**

Nicolas Elie, Antoinette Blouin, Noël Brunetière. Dynamic invariance in near field acoustic levitation. ASME Letters in Dynamic Systems and Control, 2022, 2 (1), 10.1115/1.4051141 . hal-03376601

HAL Id: hal-03376601

<https://hal.science/hal-03376601>

Submitted on 18 Oct 2021

HAL is a multi-disciplinary open access archive for the deposit and dissemination of scientific research documents, whether they are published or not. The documents may come from teaching and research institutions in France or abroad, or from public or private research centers.

L'archive ouverte pluridisciplinaire **HAL**, est destinée au dépôt et à la diffusion de documents scientifiques de niveau recherche, publiés ou non, émanant des établissements d'enseignement et de recherche français ou étrangers, des laboratoires publics ou privés.

Dynamic invariance in near field acoustic levitation

Nicolas Elie

Antoinette Blouin

Noël Brunetière *

October 18, 2021

Abstract

It is possible to levitate a mass by vibrating a flat disk located under the mass. This near-field acoustic levitation is particularly useful for eliminating friction between moving objects. This paper presents an experimental and theoretical study of the dynamic behavior of a levitating mass for different magnitudes of oscillation of the flat disk. The magnitude of the vibration of the mass appears to be independent of the amplitude of the vibration of the disk over a range of two orders of magnitude. This unusual behavior is due to the simultaneous changes of the stiffness of the air film and the natural frequency of the system as the plate vibration is changed. As the plate oscillation is reduced, the distance to resonance decreases, allowing an increase of the ratio of the output to input signals in such a way that the output remains constant. This result can be useful for improving the energy efficiency of the levitation.

1 Introduction

The non-linear dynamic behavior of mechanical systems can lead to complex and unpredictable long term behavior. This has led to the emergence of a dedicated research topic, non-linear dynamics, including chaos theory [1]. In this paper it will be shown that on the other hand, non-linear dynamic behavior can lead to very simple behavior characterized by an invariant parameter. This particular behavior has been observed in a near field acoustic levitation system composed of a horizontal plate having

an oscillating vertical motion generating a force able to levitate a mass.

Levitation has attracted the attention of physicists for a long time because of the number of its applications, including containerless processing and manipulation, frictionless bearings, and high-speed ground transportation [2]. The use of acoustic waves is one of the physical means to achieve levitation. There are two types of acoustic levitation, depending on the ratio of the levitated distance h_0 to the wave length of the sound waves [3]: A ratio higher than unity corresponds to standing waves, but when this ratio is much smaller than unity, it is near-field acoustic levitation, the topic of the present paper. Even if standing waves allow the manipulation of solids of any shape and even liquids [4], near-field acoustic levitation allows attaining a levitation force as high as 70 kN per square meter [5].

To save energy during acoustic levitation, it is usual to operate the actuator at its resonance frequency [6]. The dynamic operating condition is thus imposed by the structure of the actuator itself [7]. As a consequence, there have been very few studies focused on the dynamics of the levitated mass, except a recent paper [8]. However, this topic has been more deeply analyzed in MEMS applications where the damping due to the air film is a strong limiter of the displacement of the moving parts [9]. In this case, the mass is not levitated but elastically linked to a support. It was found by experiments [10] and theory [11, 12] that the dynamic behavior depends on the squeeze number Λ , Eq. 3. At low squeeze numbers, the damping effect is dominant, whereas at high squeeze numbers, the air film mainly behaves as a spring. As Λ is a function of the average air

*Institut Pprime CNRS, University of Poitiers - Dept GMSC - Poitiers - France - noel.brunetiere@univ-poitiers.fr

film thickness h_0 , the dynamic properties of the air film change with its thickness, making the behavior of the system non-linear. An additional non-linearity is observed at high oscillation amplitudes, due to the inertia of the air [13].

In this paper, the dynamic behavior of a levitated mass, when the vibration amplitude of the actuator is varied, is studied experimentally, numerically, and analytically.

2 Materials and methods

The experimental equipment is presented in Figure 1. A flat disk is vertically moved by a piezo-actuator (Piezomechanik PSt 150/5/7/VS10) attached to a massive frame. The oscillation frequency $f = \frac{\omega}{2\pi}$ and amplitude e of the plate are controlled. A circular mass of radius $R = 15$ mm and mass $m = 17.76$ g is placed above the plate. The surfaces of the plate and disk were polished and have a flatness defect lower than $1 \mu\text{m}$. Two optical sensors were used to measure the vertical position, h_1 , of the plate and of the disk, h_2 . Two thin wires were used to avoid any parasitic lateral movement of the disk during levitation.

Since the distance h between the mass and the plate is several orders of magnitude smaller than the radius R of the disk and the oscillation period is small compared to the time needed for sound waves to travel across the film, the air flow in the gap can be described by the Reynolds equation used for a viscous thin isothermal gas, written here in dimensionless form [14, 15]:

$$\frac{\partial}{\partial \bar{r}} \left(\bar{p} \bar{r} \bar{h}^3 \frac{\partial \bar{p}}{\partial \bar{r}} \right) = \Lambda \bar{r} \frac{\partial \bar{p} \bar{h}}{\partial \bar{t}} \quad (1)$$

Here, the dimensionless variables are

$$\bar{h} = \frac{h}{h_0}, \quad \bar{r} = \frac{r}{R}, \quad \bar{p} = \frac{p}{p_a}, \quad \bar{t} = \omega t \quad (2)$$

where p is the air pressure, p_a the ambient pressure and h_0 the average distance between the two surfaces. The ratio between the two terms of the equation is controlled by the squeeze number:

$$\Lambda = \frac{12\mu\omega}{p_a} \frac{R^2}{h_0^2}. \quad (3)$$

By numerically solving the Reynolds equation, it is possible to find the distribution of the air pressure in the gap and the resulting force. It is then possible to determine the vertical position of the mass using Newton's law.

When $\Lambda \gg 1$, the right hand side of the equation is dominant and the product of the thickness h of the air film and the pressure is constant. This means that there is no more viscous flow of the air trapped between the surfaces. It behaves as a gas submitted to the motion of an oscillating piston. It is thus possible to derive an analytical solution (see the Appendix). The average film thickness is thus

$$h_0 = \frac{e}{\sqrt{L}} + \frac{g(L+1)}{\omega^2 L} \quad (4)$$

where $L = \frac{mg}{\pi R^2 p_a}$ is the load parameter and e the plate vibration amplitude. The vibration amplitude a of the levitated mass is found to be

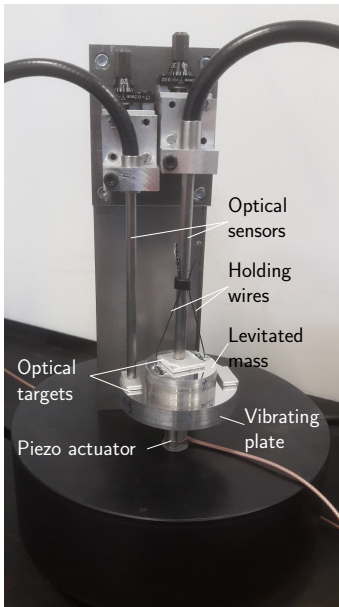
$$a = \frac{g}{\omega^2} \frac{L+1}{\sqrt{L}} \quad (5)$$

In addition to the condition on Λ , this relation is verified if $(a+e) \ll h_0$ (see the Appendix). According to this equation, the amplitude of vibration of the levitated mass is independent of the amplitude e of the input vibration, which is unusual for a dynamic system.

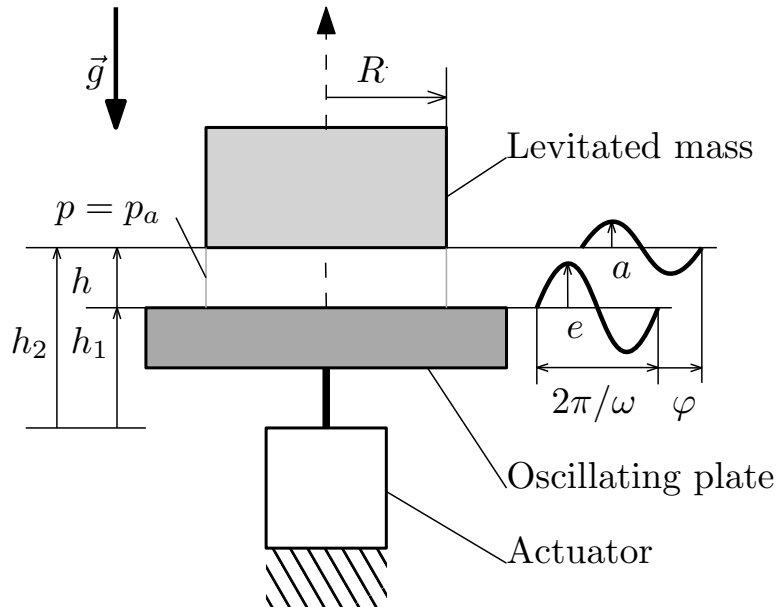
3 Results

To analyze the influence of e , that is the vibration amplitude of the plate, some tests were conducted at a frequency $f = 3500$ Hz and for e varying from $0.027 \mu\text{m}$ to $2.8 \mu\text{m}$. These values correspond to the lowest value allowing levitation during the tests and the maximum amplitude reachable by the piezo-actuator. The frequency was chosen to be far enough away from the natural vibrating frequencies of the frame of the system. The experiments were repeated four times.

Figure 2 presents the position of the vibrating plate h_1 and of the levitated mass h_2 for six different amplitudes e of the plate vibration distributed over two orders of magnitude. Note that the h_2 signal is a little noisier than h_1 due to the lower sensitivity of the



a)



b)

Figure 1: a) Picture of the test rig. The optical sensors are fiber optic sensors (Philtec D125 for the plate and D170 for the mass). The target has a controlled roughness to adapt range and sensitivity of the sensors - b) configuration of the problem showing the different parameters

sensor used for the mass, which has a higher working range. As expected, the average thickness of the air film increases with e . However, the amplitude of the vibration of the mass appears to be almost constant even if e is multiplied by 100. A similar finding has been obtained by Ilssar and Butcher by numerical simulation but over a much smaller range [8].

It is then possible to calculate the average air film thickness h_0 , the phase shift between the two signals, and the standard deviation σ of the position of the levitated mass. They are presented in Figures 3, 4 and 5, respectively, as a function of the plate vibration amplitude e . The four test results are presented as well as the results of the numerical simulations and analytical solutions.

The average film thickness obviously increases with the magnitude of the plate oscillation e . The lowest recorded film thickness was about $3 \mu\text{m}$, when the plate vibration amplitude was $0.027 \mu\text{m}$. This amplitude e is one-third that of the one predicted with the empirical relation for lift-off of Brunetière et al. [14]. The film thickness first evolves linearly with e and then the slope slightly decreases with increasing plate amplitude. The maximum film thickness reached is about $40 \mu\text{m}$. The linear evolution of h_0 is captured by both the numerical and analytical approaches with a vertical shift of respectively $4 \mu\text{m}$ and $5 \mu\text{m}$. The difference between the numerical simulation and the experiments decreases and tends to a perfect correlation when h_0 is higher than $20 \mu\text{m}$. Below this value, the Knudsen number (ratio of the free mean path of the gas to the film thickness) Kn is lower than 0.0033, indicating that there could occur a transition to a slip flow due to gas rarefaction. This effect is not considered in the model. The analytical model predicts a linear increase of the film, which is not in agreement with experimental observation. Indeed, when the film thickness is increased, the squeeze number Λ is strongly decreased, rendering invalid the assumption used to build the model. The deviation from the linear evolution is due to the viscous flow of the gas in the gap between the plate and the mass.

The phase shift φ between the plate and the mass oscillation is presented in Figure 4 as a function of e . Except for a few experimental results obtained at the

lowest values of e , the phase shift is less than $-\pi/2$, indicating that the air-film-mass system is working at a frequency above its natural frequency. The few outliers could be due to uncertainty in the phase calculation of the input signal due to the large ratio between the noise and the signal obtained at low e (see Figure 2). The experimental and numerical results are very consistent with a decrease from about $-\pi/2$ at low e before reaching a minimum for $e \simeq 0.3 \mu\text{m}$. The phase shift then rises slightly to about $-3\pi/2$. The analytical model does not consider any damping, and thus leads to a constant phase $-\pi$ over the entire range.

The standard deviation σ of the displacement of the mass is presented in Figure 5 as a function of e . Two sets of experimental results are presented. The shaded one corresponds to the standard deviation calculated on the raw signal and in the second set the noise of the sensor, equal to $0.125 \mu\text{m}$ RMS, was subtracted. As previously seen in Figure 2, the amplitude of the vibration of the mass is impressively insensitive to the input signal e , even when varying over a range of two orders of magnitude. For e lower than $0.5 \mu\text{m}$, there is a discrepancy on the test results due to occurrence of condensation drops between the surfaces due to the very low distance between the surfaces. The numerical simulations highlight a slight decrease of σ with e and a quite good agreement with the tests. The analytical model (Eq. 5) gives a constant value about 30% higher than the test average results. The almost constant value of the mass amplitude vibration is obtained experimentally and theoretically.

4 Discussion

Assuming that the air film can be described by a stiffness coefficient and a damping coefficient, it is possible to identify the natural frequency or pulsation ω_0 of the system that is thus reduced to a mass-spring-damper system:

$$\left(\frac{\omega_0}{\omega}\right)^2 = \frac{1}{1 - \cos \varphi \frac{e}{\sigma\sqrt{2}}} \quad (6)$$

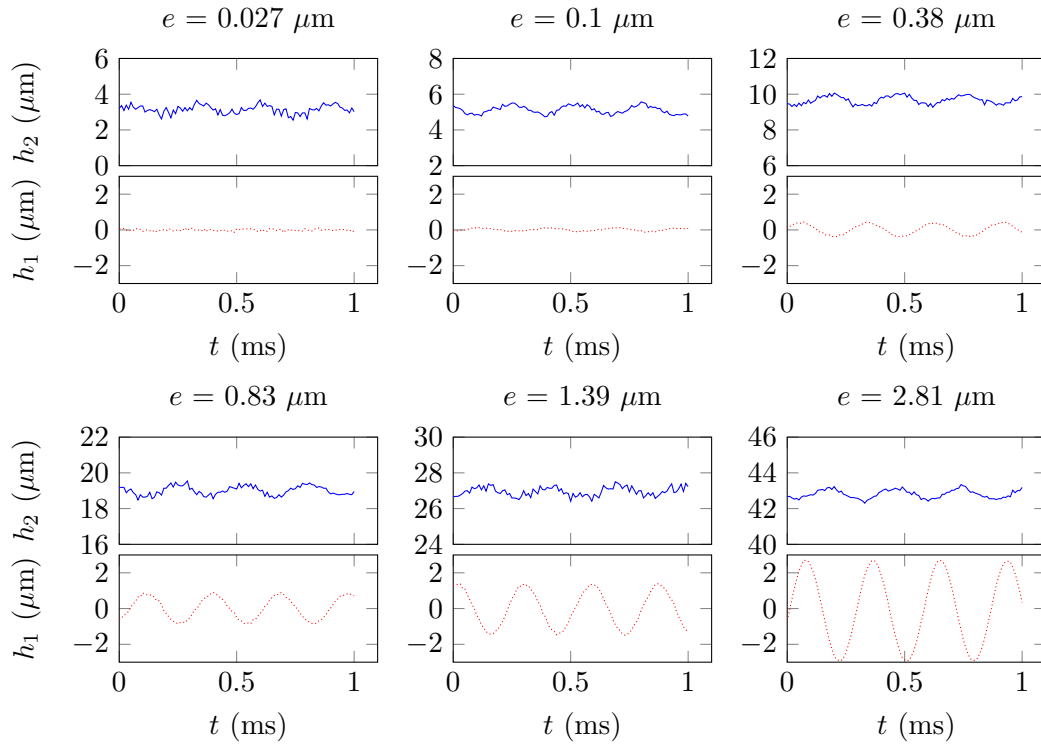


Figure 2: Motion of the vibrating plate (dotted) at six different amplitudes e and corresponding levitated mass motion (solid) as a function of time. The vibration frequency is $f = 3500$ Hz and the mass of the levitated object is $m = 17.76$ g

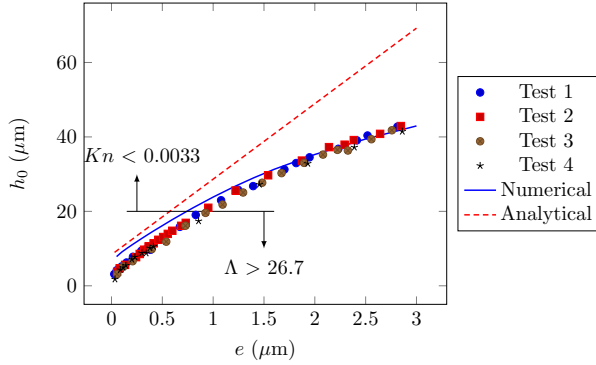


Figure 3: Average film thickness h_0 over one period as a function of the plate vibration amplitude e : Results of four different test series, simulation results and analytical solution (Eq. 4).

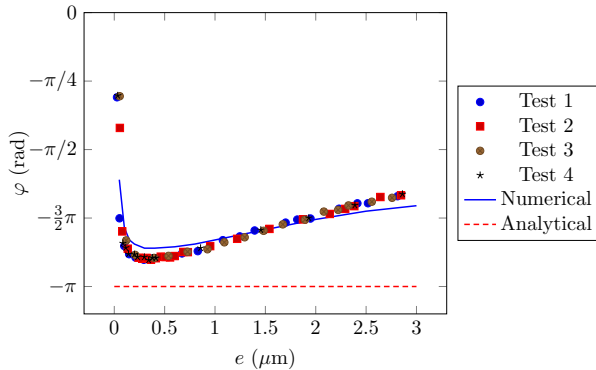


Figure 4: Phase shift between the position h_2 of the levitated mass and the position h_1 of the plate as a function of the amplitude e of the vibration of the plate: Results of four different test series, simulation results, and analytical solution.

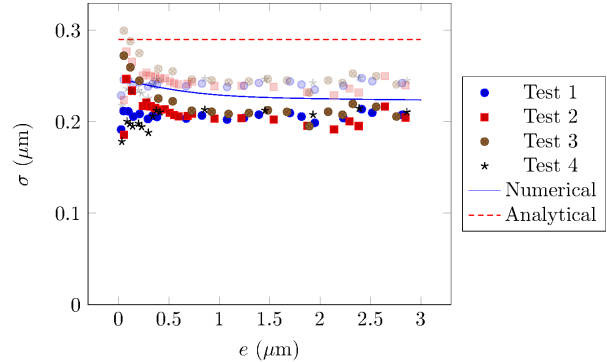


Figure 5: Standard deviation σ of the levitated mass position h_2 as a function of the plate vibration amplitude e : Results of four different test series (shaded points correspond to raw results σ_r and solid points to results after noise removal: $\sigma = \sqrt{\sigma_r^2 - 0.125(\mu m)^2}$, simulation results and analytical solution (Eq. 5).

The square of the ratio of the natural frequency to the operating frequency is presented as a function of e . This ratio is linked to the stiffness k of the air film $(\frac{\omega_0}{\omega})^2 = \frac{k}{m\omega^2}$. The three approaches give very similar results with a ratio that decreases from about 1 to 0.1 when e is varied from 0.027 to 2.8 μm (see Figure 6). Even if the analytical solution leads to a higher value of σ and $\cos \varphi$, their ratio is probably close to the experimental and numerical values. The variation of $(\frac{\omega_0}{\omega})^2$ means that when the amplitude of the vibration of the plate is decreased, the stiffness of the film is increased due to the lower film thickness. In the case of the entrapped air assumption (analytical approach), it can be shown that $k \propto h_0^{-2}$. This increase in stiffness makes the natural pulsation closer to the operating pulsation. As the system is working closer to its resonance, it is possible to maintain the vibration amplitude of the mass at a constant value by amplifying the input signal, thanks to the resonance. The reason why the natural frequency varies in such a way that the amplitude of the vibration of the mass is kept almost constant is difficult to explain based on the experimental results and numerical simulations. The analytical model, even if not accurate for a description of the problem over the entire range,

can provide a simple explanation of this phenomenon (see the Appendix). The oscillating part of the force generated in the air film is proportional to $\frac{b}{h_0}$, where b is the amplitude of the air gap vibration (including e and a). This force component must balance the acceleration of the mass that is proportional to a or σ . Thus $a \propto \frac{b}{h_0}$. To ensure a mass balance over one period of the oscillation of the gas entering and exiting the gap, it can be shown that an average overpressure proportional to $\left(\frac{b}{h_0}\right)^2$ is needed. Since this average overpressure must balance the load due to the mass of the levitated disk, it is independent of e . Thus, as the mass is kept constant, $\frac{b}{h_0}$ and then a are invariant and independent of e . In the real problem, the explanation is more complex, as there is a contribution of the viscous flow to the levitation force as well as rarefaction effects at low Knudsen numbers.

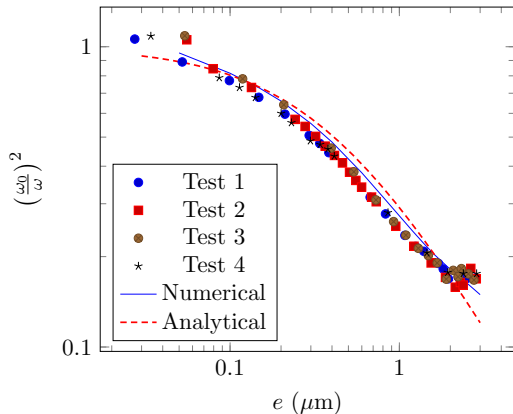


Figure 6: Square of the ratio of the critical pulsation ω_0 to operating pulsation ω as a function of the plate vibration amplitude e : Results of four different test series, simulation results and analytical solution. The results were calculated with Eq. (6).

5 Conclusion

The dynamics of a metallic disk maintained in levitation by near-field acoustic waves has been experimentally studied when the amplitude of vibration of the actuated plate is varied over a range of two orders

of magnitude. That study has been complemented with numerical simulations and an analytical model. It has been found both experimentally and theoretically that the amplitude of vibration of the levitated mass is almost independent of the magnitude of the oscillation of the plate due to the simultaneous variation of the stiffness of the film and the natural frequency of the system. This is an illustration of how non-linear dynamics can lead to a simple behavior. In addition, these findings indicate that it is possible to operate the levitation process with a very low energy input as the amplitude e of the plate vibration can be a few tens of nanometers due to the proximity with the resonance of the system. This is however accompanied by a decrease in film thickness h_0 .

Acknowledgment

This work pertains to the French government program Investissements d’Avenir (LABEX INTERACTIFS, reference ANR-11-LABX-0017-01 and EUR INTREE ANR-ANR-18-EURE-0010).

References

- [1] Strogatz, S. H., 2018. *Nonlinear dynamics and chaos with student solutions manual: With applications to physics, biology, chemistry, and engineering*. CRC press.
- [2] Brandt, E., 1989. “Levitation in physics”. *Science*, **243**(4889), pp. 349–355.
- [3] Vandaele, V., and Lambert, P. and Delchambre, A., 2005. “Non-contact handling in microassembly: Acoustical levitation”. *Precision Engineering*, **29**(4), October, pp. 491–505.
- [4] Xie, W., Cao, C., Lü, Y., and Wei, B., 2002. “Levitation of iridium and liquid mercury by ultrasound”. *Physical review letters*, **89**(10), p. 104304.
- [5] Ueha, S., Hashimoto, Y., and Koike, Y., 2000. “Non-contact transportation using near-

- field acoustic levitation”. *Ultrasonics*, **38**(1), pp. 26 – 32.
- [6] Gabay, R., and Bucher, I., 2006. “Resonance tracking in a squeeze-film levitation device”. *Mechanical systems and signal processing*, **20**(7), pp. 1696–1724.
- [7] Stolarski, T., 2006. “Self-lifting contacts: From physical fundamentals to practical applications”. *Proceedings of the Institution of Mechanical Engineers, Part C: Journal of Mechanical Engineering Science*, **220**(8), pp. 1211–1218.
- [8] Ilssar, D., and Bucher, I., 2017. “The effect of acoustically levitated objects on the dynamics of ultrasonic actuators”. *Journal of Applied Physics*, **121**(11), p. 114504.
- [9] Bao, M., and Yang, H., 2007. “Squeeze film air damping in mems”. *Sensors and Actuators A: Physical*, **136**(1), pp. 3 – 27. 25th Anniversary of Sensors and Actuators A: Physical.
- [10] Andrews, M., Harris, I., and Turner, G., 1993. “A comparison of squeeze-film theory with measurements on a microstructure”. *Sensors and Actuators A: Physical*, **36**(1), pp. 79 – 87.
- [11] Blech, J., 1983. “On isothermal squeeze films”. *Journal of Lubrication technology*, **105**(4), October, pp. 615–620.
- [12] Crandall, I. B., 1918. “The air-damped vibrating system: Theoretical calibration of the condenser transmitter”. *Phys. Rev.*, **11**, Jun, pp. 449–460.
- [13] Huang, S., Borca-Tasciuc, D.-A., and Tichy, J., 2014. “Limits of linearity in squeeze film behavior of a single degree of freedom microsystem”. *Microfluidics and nanofluidics*, **16**(6), pp. 1155–1163.
- [14] Brunetiere, N., Blouin, A., and Kastane, G., 2018. “Conditions of lift-off and film thickness in squeeze film levitation”. *Journal of Tribology*, **140**, May, p. 031705 (6 pages).
- [15] Brunetiere, N., and Wodtke, M., 2020. “Considerations about the applicability of the reynolds equation for analyzing high-speed near field levitation phenomena”. *Journal of Sound and Vibration*, p. 115496.

Appendix A: Analytical model

Geometrical configuration

The configuration of the problem is presented in Figure 1. A circular plate is oscillating vertically at a frequency $f = \frac{\omega}{2\pi}$ and an amplitude e thanks to an actuator. The vertical position of the top surface of the oscillating plate is given by:

$$h_1 = e \sin(\omega t + \phi) \quad (7)$$

A cylindrical mass of radius R and mass m is placed on the top of the vibrating plate. If the oscillating frequency and amplitude of the plate are high enough, the mass will be in levitation above the plate. The mass is assumed to vibrate at the same frequency as the plate. The vertical position of the bottom surface of the levitated mass can thus be described in this way:

$$h_2 = h_0 + a \sin(\omega t + \psi) \quad (8)$$

The thickness of the air film is thus:

$$h = h_2 - h_1 \quad (9)$$

The phase ϕ of the plate is chosen so that :

$$a \sin \psi - e \sin \phi = 0 \quad (10)$$

$$a \cos \psi - e \cos \phi = b > 0 \quad (11)$$

The film thickness is then:

$$h = h_0 + b \sin(\omega t) \quad (12)$$

Pressure in the fluid film

It is assumed that $h \ll R$ and the lubrication assumption are verified. The pressure in the air film is thus

governed by the Reynolds equation. The pressure is thus independent of the vertical coordinate and just varies with time and radial position $p = p(r, t)$. The relative magnitude of the transient term of the Reynolds equation is controlled by the squeeze number:

$$\Lambda = \frac{12\mu\omega R^2}{p_a h_0^2} \quad (13)$$

where μ is the viscosity of air and p_a the atmospheric pressure. If we assume that $\Lambda \gg 1$ then the pressure is given by the following equation:

$$\frac{\partial p h}{\partial t} = 0 \quad (14)$$

This equation can be time integrated:

$$p = \frac{C}{h} \quad (15)$$

where C is an unknown constant. This pressure evolution is known as the Boyle's law. In this case $p = p(t)$. It is like if an amount of air is compressed and stretched when the film thickness varies without escaping from the air gap. The air film is equivalent to a pure spring. In the general case where the air can flow and escape ($\Lambda \not\gg 1$), there is a dissipation due to viscosity and the film is equivalent to a spring and a damper.

It is sometimes assumed that the pressure is equal to p_a when $h = h_0$, giving $C = p_a h_0$. In the present work we will use a more general case $C = \alpha p_a h_0$ where α has to be determined.

Determination of α

The Boyle's law pressure distribution is not realistic close to the edge of the air film. Indeed the real pressure profile in the air film must connect to the ambient pressure at the outer radius R . An illustration of the pressure profile is given in Figure 7.

The following assumptions are used. The width ℓ of the pressure variation zone is small compared to the outer radius: $\ell \ll R$. In addition, there is no flow between this zone and the central zone where the pressure is given by the Boyle's law. Thus the pressure derivative is zero at this boundary. Using a

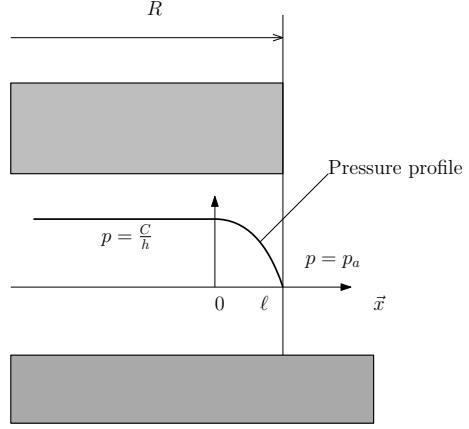


Figure 7: Air pressure at the edge of the film

local coordinate x defined in Figure 7, the pressure profile is:

$$p(x) = \frac{p_a - \frac{C}{h}}{\ell^2} x^2 + \frac{C}{h} \quad (16)$$

This equation verifies $p(\ell) = p_a$ and $\frac{\partial p}{\partial x}(0) = 0$.

The radial mass flow rate of air is given by:

$$\dot{m} = \frac{\pi r h^3}{12\mu} \rho \frac{\partial p}{\partial x} \quad (17)$$

To ensure a constant mass of air in the central zone, the integral of the mass flow at the outer radius over a period must be zero:

$$\int_0^T \dot{m}(\ell) dt = 0 \quad (18)$$

Considering only the time varying terms and the pressure profile expression, the following relation must be verified:

$$\int_0^T h^3 \frac{\partial p}{\partial x}(\ell) dt = \frac{2}{\ell^2} \int_0^T (p_a h^3 - C h^2) dt = 0 \quad (19)$$

When integrating power function of h , only constant term and square of sine function give non-zero values after integration. The following relation is obtained:

$$p_a \left(h_0^3 + \frac{3}{2} b^2 h_0 \right) - C \left(h_0^2 + \frac{b^2}{2} \right) = 0 \quad (20)$$

The pressure constant C is thus:

$$C = \frac{p_a h_0 \left(1 + \frac{3b^2}{2h_0^2} \right)}{1 + \frac{b^2}{2h_0^2}} \quad (21)$$

A new assumption can be useful. It is assumed that the average film thickness h_0 is much higher than the amplitude of vibration b . Thus a Taylor development of the numerator can be done:

$$C = p_a h_0 \left(1 + \frac{3b^2}{2h_0^2} \right) \left(1 + \frac{b^2}{2h_0^2} + O \left(\frac{b^4}{h_0^4} \right) \right) \quad (22)$$

If only second order terms are considered, the pressure constant is finally:

$$C = p_a h_0 \left(1 + \frac{b^2}{h_0^2} \right) \quad (23)$$

Using C to get α :

$$\alpha = \frac{C}{p_a h_0} = 1 + \frac{b^2}{h_0^2} \quad (24)$$

Equation of motion of the levitated mass

The levitated mass is subjected to the following forces:

- The weight $-mg$
- The air pressure on the top surface $-\pi R^2 p_a$
- The air pressure in the film $F_f = \pi R^2 p_a h_0 \frac{\alpha}{h}$

The film force can be expressed as:

$$F_f = \pi R^2 p_a \frac{\alpha}{1 + \frac{b}{h_0} \sin(\omega t)} \quad (25)$$

Remembering that $\frac{b}{h_0} \ll 1$, the force equation can be simplified using a Taylor expansion at the first order:

$$F_f = -\pi R^2 p_a \alpha \left[1 - \frac{b}{h_0} \sin(\omega t) \right] \quad (26)$$

The Newton's law applied to the levitated mass gives:

$$\pi R^2 p_a \alpha \left[1 - \frac{b}{h_0} \sin(\omega t) \right] - \pi R^2 p_a - mg = -m a \omega^2 \sin \sin(\omega t + \psi) \quad (27)$$

By identification and using that $b > 0$ and $a > 0$ the following equations are obtained:

$$\alpha - 1 = \frac{mg}{\pi R^2 p_a} = L \quad (28)$$

$$\psi = 0 \quad (29)$$

$$\alpha \frac{b}{h_0} = L a \frac{\omega^2}{g} \quad (30)$$

where L is the load parameter. Using equations 28 and 24, the ratio of the vibration amplitude and average film thickness is obtained:

$$\frac{b}{h_0} = \sqrt{L} \quad (31)$$

From equations 29 and 10, it is found that $\phi = 0$ or $\phi = \pi$.

Finally, the magnitude of the levitated mass can be expressed by replacing α and $\frac{b}{h_0}$ by their expressions:

$$a = \frac{g}{\omega^2} \frac{L+1}{\sqrt{L}} \quad (32)$$

It is now possible to express the average film thickness:

$$h_0 = \frac{b}{\sqrt{L}} = \frac{a - e \cos \phi}{\sqrt{L}} \quad (33)$$

If $\phi = 0$, it is necessary that $a > e$ to have a positive film thickness. If $\phi = \pi$ there is no specific condition. The following relations are obtained:

$$h_0 = -\frac{e}{\sqrt{L}} + \frac{g(L+1)}{\omega^2 L} \quad \text{for } \phi = 0 \quad (34)$$

$$h_0 = \frac{e}{\sqrt{L}} + \frac{g(L+1)}{\omega^2 L} \quad \text{for } \phi = \pi \quad (35)$$

The first solution (Eq. 34) corresponds to a phase shift of 0 and thus to an operating frequency lower than the natural frequency of the system. In this

case the film thickness decreases when the amplitude of the input vibration is increased. This solution is not experimentally observed (see experiments in the paper). The second solution (Eq. 35) corresponds to an operating frequency higher than the natural frequency of the system ($\phi = \pi$). In this case, the levitation height increases with e as experimentally observed. This second solution will be used.